

## Phase A Design of the LUMIO Spacecraft: a CubeSat for Observing and Characterizing Micro-Meteoroid Impacts on the Lunar Far Side

Cervone, A.; Topputo, Francesco; Speretta, S.; Menicucci, A.; Biggs, Juliet; Di Lizia, P.; Massari, M.; Franzese, V.; Giordano, C; More Authors

**Publication date**

2020

**Document Version**

Accepted author manuscript

**Published in**

71st International Astronautical Congress (IAC)

**Citation (APA)**

Cervone, A., Topputo, F., Speretta, S., Menicucci, A., Biggs, J., Di Lizia, P., Massari, M., Franzese, V., Giordano, C., & More Authors (2020). Phase A Design of the LUMIO Spacecraft: a CubeSat for Observing and Characterizing Micro-Meteoroid Impacts on the Lunar Far Side. In *71st International Astronautical Congress (IAC): The CyberSpace Edition, 12-14 October 2020* [IAC-20-B.4.8.1] IAF/AIAA.

**Important note**

To cite this publication, please use the final published version (if applicable).  
Please check the document version above.

**Copyright**

Other than for strictly personal use, it is not permitted to download, forward or distribute the text or part of it, without the consent of the author(s) and/or copyright holder(s), unless the work is under an open content license such as Creative Commons.

**Takedown policy**

Please contact us and provide details if you believe this document breaches copyrights.  
We will remove access to the work immediately and investigate your claim.

## Phase A Design of the LUMIO Spacecraft: a CubeSat for Observing and Characterizing Micro-Meteoroid Impacts on the Lunar Far Side

A. Cervone<sup>(1)\*</sup>, F. Topputo<sup>(2)</sup>, S. Speretta<sup>(1)</sup>, A. Menicucci<sup>(1)</sup>, J. Biggs<sup>(2)</sup>, P. Di Lizia<sup>(2)</sup>, M. Massari<sup>(2)</sup>, V. Franzese<sup>(2)</sup>, C. Giordano<sup>(2)</sup>, G. Merisio<sup>(2)</sup>, D. Labate<sup>(3)</sup>, G. Pilato<sup>(3)</sup>, A. Taiti<sup>(3)</sup>, E. Bertels<sup>(4)</sup>, B. Bosman<sup>(4)</sup>, K. Woroniak<sup>(4)</sup>, J. Rotteveel<sup>(4)</sup>, A. Thorvaldsen<sup>(5)</sup>, A. Kukharenska<sup>(5)</sup>, N. Prieur<sup>(5)</sup>, J. Vennekens<sup>(6)</sup>, R. Walker<sup>(6)</sup>

<sup>(1)</sup> TU Delft, Kluyverweg 1, 2629 HS, Delft, The Netherlands

<sup>(2)</sup> Politecnico di Milano, Via La Masa 34, 20156, Milano, Italy

<sup>(3)</sup> Leonardo, Via delle Officine Galileo 1, 50013, Campi Bisenzio, Firenze, Italy

<sup>(4)</sup> ISIS-Innovative Solutions in Space, Motorenweg 23, 2623 CR, Delft, The Netherlands

<sup>(5)</sup> Science and Technology AS, Tordenskiolds Gate 6, 0160, Oslo, Norway

<sup>(6)</sup> ESA/ESTEC, Keplerlaan 1, 2201 AZ, Noordwijk, The Netherlands

\* Corresponding Author

### Abstract

The Lunar Meteoroid Impacts Observer (LUMIO) is a CubeSat mission to a halo orbit at Earth–Moon  $L_2$  that shall observe, quantify, and characterize meteoroid impacts on the Lunar farside, by detecting their flashes. In this way, LUMIO is expected to significantly contribute to Lunar Situational Awareness and to the current knowledge on the evolution of meteoroids in the cislunar space. This will allow, ultimately, to achieve a better understanding of the origins of the Solar System, the composition of its planets and the possible hazards caused by impacts between the Earth and Near Earth Objects.

LUMIO was one of the proposals submitted to the SysNova Lunar CubeSats for Exploration call by the European Space Agency. The mission was awarded ex-aequo winner of the challenge, and its scientific relevance and technical feasibility were confirmed by an independent study conducted by the ESA Concurrent Design Facility. The LUMIO Phase A study is currently ongoing and is scheduled for completion by the end of 2020.

This paper, after providing a short overview of the scientific relevance of the mission, presents in detail the status of the current LUMIO Phase A study, including an overview of all spacecraft sub-systems and the evolution of their design from Phase 0 to Phase A.

**Keywords:** LUMIO, Interplanetary CubeSat missions, Meteoroid impacts, Lunar Situational Awareness, ESA SysNova challenge

### 1. Introduction

LUMIO (Lunar Meteoroid Impacts Observer) is a CubeSat mission to a halo orbit at Earth–Moon  $L_2$  that shall observe, quantify, and characterize meteoroid impacts on the Lunar farside by detecting their flashes, complementing Earth-based observations on the Lunar nearside, to provide global information on the Lunar Meteoroid Environment and contribute to Lunar Situational Awareness.

LUMIO was one of the proposals submitted to the SysNova Lunar CubeSats for Exploration (LUCE) call by the European Space Agency (ESA), a challenge intended to generate new and innovative concepts and to verify quickly their usefulness and feasibility via short concurrent studies [1]. After the first phase of the challenge (open call for ideas), LUMIO was one of the four proposals selected for performing a pre-Phase 0 analysis, funded by ESA. During the final review and

evaluation from ESA, the mission was then selected as one of the two ex-aequo winners of the challenge. As prize for the winners, ESA offered the opportunity to perform an independent study in its Concurrent Design Facility (CDF), to further assess the objectives, design and feasibility of the mission. The CDF study confirmed the feasibility and the scientific value of the mission [2], proposing a number of design iterations that, together with the initial design proposed by the LUMIO team in response to the SysNova challenge, contributed to form the Phase 0 study of the mission. Details on this Phase 0 study have been provided by the LUMIO team in numerous publications and presentations, see for example [3], [4], [5].

The LUMIO Phase A study, funded by ESA under the General Support Technology Programme (GSTP), through the support of the national delegations of Italy (ASI), the Netherlands (NSO) and Norway (NOSA), has

been kicked off in March 2020 and is scheduled for completion by the end of 2020.

This paper will present the scientific relevance of LUMIO, its mission analysis and spacecraft design, highlighting the steps taken from Phase 0 to the current Phase A work.

## 2. Scientific relevance

Near Earth Objects (NEO) are asteroids or comets with a perihelion of less than 1.3 AU. As of September 2020, the Minor Planet Centre database lists more than 23,900 NEO discovered so far [6]. NASA's Near-Earth Object Program database estimates that around 900 of these NEO are larger than 1 km, and more than 9,000 of them are larger than 140 m [7]. These bodies represent remnant debris from the formation of our Solar System and, as such, provide crucial information to understand the composition of planets and, more in general, the Solar System. Furthermore, impacts of NEO with the Earth are events that can cause a wide range of catastrophic consequences, from a humanitarian crisis to, potentially, the extinction of life on our planet. It is therefore very important to invest resources to better understand and, possibly, predict these events.

Telescopic observations allow to detect NEO in the range from 1 km (or bigger) down to 1 meter in size, but typically fail in providing an accurate monitoring of the sub-meter meteoroid population, for which few direct observation methods are currently known. These meteoroids are small Sun-orbiting fragments of asteroids and comets, formed as a consequence of asteroid collisions or release of dust particles from comets, with size ranging from micrometers to meters and mass ranging from  $10^{-15}$  to  $10^4$  kg [8]. Meteoroids are hardly detectable in a direct way, but can be observed indirectly from other phenomena, such as their impact with a celestial body. When dispersed along the same orbit, they form a meteoroid *stream*, while a cluster of meteoroids at the same orbital longitude is called a meteoroid *swarm* and, when colliding with a celestial body, originates a meteoroid *shower*. The development of meteoroid impact flux models is therefore crucial for the sustainable development of space assets and, for smaller particles (*micrometeoroids*, with size in the range from 10  $\mu\text{m}$  to 2 mm), also represent an important contribution to the study of space weather.

A large amount of meteoroids and micrometeoroids continuously enter the Earth–Moon system, becoming a potential threat and causing, in particular, substantial modifications of the Lunar surface, as shown for example by recent observations from the Lunar Reconnaissance Orbiter Camera [9]. There are also various hypothesis and speculations on possible asymmetries in the spatial distribution of impacts across the Lunar surface [10]. It is theorized that the Lunar

nearside has approximately 0.1% more impacts than the farside, due to the influence of the Earth gravity field; the equatorial flux is expected to be 10–20% larger than the polar regions, due to the higher number of large meteoroids in low orbital inclinations; and the Lunar leading side (apex) encounters between 37 and 80% more impactors than the trailing side (antapex), due to the Moon synchronous rotation. In a lunar meteoroid impact, the kinetic energy of the impactor is partitioned into: the generation of a seismic wave; the excavation of a crater; the ejection of particles; the emission of radiation through flashes. Although in principle any of these phenomena can be observed to detect Lunar meteoroid impacts, the detection of impact flashes has been selected by LUMIO as the most advantageous method since it yields an independent detection of meteoroid impacts, provides the most complete information about the impactor, and allows for the monitoring of a large Moon surface area.

Light flashes at the Moon are typically observed by detecting a local spike of the luminous energy in the visible spectrum. If this observation is done through an Earth-based telescope, it is affected by background noise caused by the Earthshine (Earth reflected light on the Moon surface) and by thermal emissions of the Moon surface in the infrared spectrum. This problem can be partially overcome by looking at the Lunar night side, as shown by the observations of the first unambiguous lunar meteoroid impact flashes during the Leonid meteoroid showers in 1999 [11]. Several dedicated monitoring programs were initiated thereafter, including one at the NASA Marshall Space Flight Center [12] and a more recent one, NELIOTA, started in 2017 under ESA funding [13]. However, it is clear to the scientific community that Earth-based monitoring of impact flashes inherently imposes restrictions (such as the attenuation caused by atmosphere and clouds, the restrictions in observing the full disk at all longitudes, the presence of a day/night cycle and of the Earthshine), that can be avoided if the same investigation is conducted with space-based assets.

When the Earth, during its revolution around the Sun, intercepts a meteoroid swarm, the meteoroids in the swarm collide with our planet and burn in its atmosphere, giving origin to a meteor shower. The Moon is orbiting the Earth with a revolution period of 27.32 days with respect to the inertial space, and thus intercepts the same meteoroid swarms at approximately the same time. However, since the Moon has no significant atmosphere, the impacts originate in this case a meteoroid shower. The Moon spin–orbit motion is locked into a 1:1 resonance, meaning that an observer on Earth always sees the same portion of the Moon (the Lunar nearside). This obviously further constrains the observations taken from the Earth, limiting them to half of the Lunar surface. Since the Moon orbital period

relative to the Sun is 29.53 days, the illumination of the Lunar nearside varies with time, originating the Moon phases (Fig. 1). The Lunar impact flashes can only be observed from ground on the Lunar nightside, when the nearside is less than 50% illuminated, and during the Earth night. Similar limitations exist when observing the Lunar farside, but allowing in this case observations during the opposite period of the month as compared to Lunar nearside ones. The dashed green line in Fig.1 shows the portion of the Moon orbit where Earth-based observations of the nearside can be made, while the solid blue line shows the portion of the Moon orbit where space-based observations of the farside can be made. It is clear from the figure the complementarity, in both space and time, of the two types of observations.

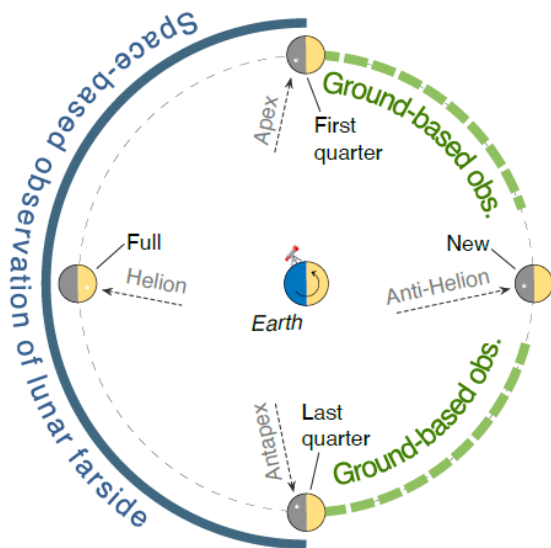


Fig. 1. Moon phases and main direction of incoming meteoroids in the Earth-Moon system.

Based on the above scientific needs and opportunities, the science question that LUMIO intends to answer is: *what are the spatial and temporal characteristics of meteoroids impacting the Lunar surface?* The corresponding science goal will be to *advance the understanding of how meteoroids evolve in the cislunar space by observing the flashes produced by their impacts with the Lunar surface.*

The range of interest for the monitoring that will be performed by LUMIO derives from the already existing observation data (see for example [14], [15]), which show no recorded events in the equivalent kinetic energy range at the Earth from  $10^{-4}$  to  $10^{-1}$  kton TNT, and significant uncertainties and error margins in the equivalent kinetic energy range at the Earth from  $10^{-6}$  to  $10^{-4}$  kton TNT. A selection of the main science requirements of LUMIO, based on the above considerations, is presented in Table 1.

Table 1. Main science requirements of LUMIO.

ID	Requirement	Rationale
SCI.010	The mission shall perform observations of the Lunar farside.	<i>Observing the lunar farside yields unique high quality science products due to the lack of Earthshine.</i>
SCI.020	The mission shall detect new meteoroid impacts to the Moon in the equivalent kinetic energy range at the Earth from $1e-4$ to $1e-1$ kton TNT.	<i>No events have ever been recorded in this range (see [14], [15]).</i>
SCI.030	The mission shall quantify the luminous energy of meteoroid impacts to the Moon in the equivalent kinetic energy range at the Earth from $1e-6$ to $1e-4$ kton TNT.	<i>Observations in this range ([14], [15]) have significant error margins, also a set of discrepancies is observed.</i>

### 3. Mission analysis and phases

LUMIO will make use of a 12U CubeSat which carries the LUMIO-Cam, an optical instrument capable of detecting light flashes in the visible spectrum to continuously monitor and process the data. The mission implements a novel orbit design and COTS CubeSat technologies, to serve as a pioneer in demonstrating how CubeSats can become a viable tool for interplanetary science and exploration. Figure 2 shows a simplified representation of the mission profile and phases.

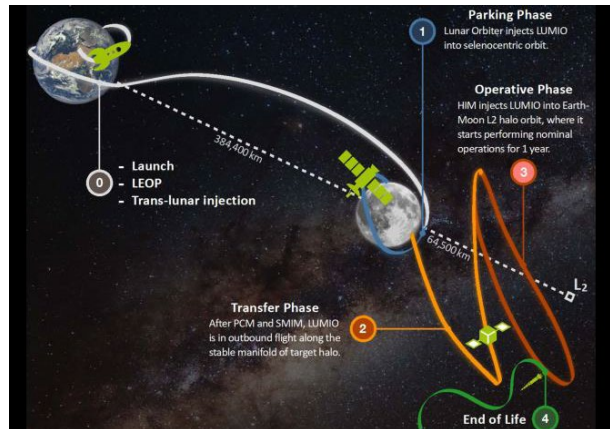


Fig. 2. LUMIO mission concept and phases.

As illustrated by Fig. 2, the mission is divided in 5 phases:

- **Earth-Moon transfer.** In this phase, after the launch, the LUMIO spacecraft will be carried inside its mothership to the Lunar parking orbit. During the transfer the spacecraft will be switched off inside its deployer and a power connection with the mothership will keep the LUMIO batteries charged.

- **Parking.** In this phase, the LUMIO spacecraft will be released in its Lunar parking orbit by the mothership. After de-tumbling and deployment of the solar arrays, the payload and all sub-systems will be commissioned. The spacecraft will cruise with radiometric navigation strategy and Direct-To-Earth communication and perform, when necessary, station keeping and wheel desaturation maneuvers.
- **Transfer.** In this phase, the LUMIO spacecraft will autonomously transfer from the parking orbit to its final operative orbit. A total of four maneuvers are expected during the transfer: a Stable Manifold Injection Maneuver (SMIM), two TCM maneuvers, and a Halo Injection Maneuver (HIM). Also in this case, the spacecraft will cruise with radiometric navigation strategy and Direct-To-Earth communication and perform, when necessary, wheel desaturation maneuvers.
- **Operative phase.** In this phase, expected to have a duration of at least 1 year, the LUMIO spacecraft will accomplish its scientific objectives. It will be divided in two sub-phases: the science cycle, during which the scientific data (images) will be continuously acquired, processed and compressed; and the navigation & engineering cycle, during which radiometric navigation base on Direct-To-Earth link will be performed (in parallel with the demonstration of an autonomous optical navigation experiment using the LUMIO-Cam) and, eventually, station keeping and wheel desaturation maneuvers will be conducted. With reference to Fig. 1, the science cycle will take place during the portion of the Lunar cycle when the illumination of the Moon allows for scientific observations (solid blue line), while the navigation & engineering cycle will take place when scientific observations of the Lunar farside are not possible (dashed green line).
- **End-of-Life.** During this final phase, all spacecraft systems will be de-commissioned, and the end of life maneuvers will be performed.

For what concerns the transfer phase, the trajectory proposed during Phase 0 was based on an injection orbit of 200x15,000 km around the Moon, later modified during the CDF study to a 600x20,000 km one in order to reduce the magnitude of the SMIM maneuver. In the Phase A study, two alternative launch opportunities are being investigated: the Commercial Lunar Payload Services (CLPS) and Artemis-2, both from NASA, with the latter representing the worst-case scenario for the transfer phase and therefore being used for the determination of the Delta-V budget that will be presented here.

The selected LUMIO operative orbit is a quasi-periodic halo orbit around Earth–Moon  $L_2$ , characterised by a Jacobi constant  $C_j = 3.09$ . This orbit was selected

from a set of 14 candidates after a thorough trade-off analysis performed during the Phase 0 study. The trajectory of this operative orbit during the expected mission time frame is shown in Fig. 3. One important advantage offered by this orbit is the absence of any eclipse periods during the complete 1-year nominal mission lifetime.

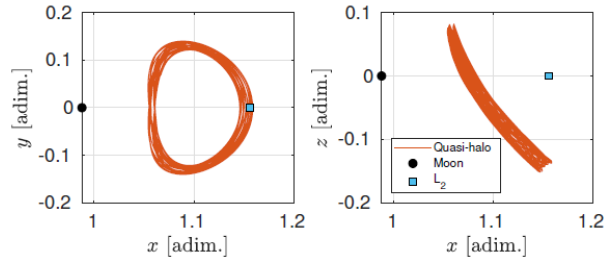


Fig. 3. Projections in the Roto-Pulsating Frame of the LUMIO operative orbit around Earth-Moon  $L_2$ .

The worst-case Delta-V budget for the LUMIO spacecraft, based on the Artemis-2 launch opportunity and an optimized transfer strategy from the corresponding release orbit, is based on a combination of deterministic and stochastic maneuvers as reported in Table 2. In this case, since the LUMIO spacecraft would be released in a trans-Lunar orbit, a completely different transfer strategy has been considered as compared to the one previously used for the Phase 0 study (and for the CLPS case). This strategy includes a set of 6 impulsive maneuvers ( $\Delta v_0$ - $\Delta v_5$ ) followed by a single TCM maneuver and by the HIM. Note, finally, that the optimized Delta-V budget that has been estimated for the CLPS case is significantly lower (116.3 m/s margined, as opposed to the 199.8 m/s of the Artemis-2 case) mainly as a consequence of its SMIM maneuver, significantly less demanding than the 6 impulsive maneuvers of the Artemis-2 case. This means that, in case the CLPS option is used as launch opportunity for LUMIO, a significantly larger Delta-V will be available on the spacecraft, allowing as an example for a longer mission lifetime in the operative orbit.

Table 2. Current worst-case Delta-V budget for LUMIO (based on the Artemis-2 launch opportunity).

Maneuver	Deterministic $\Delta v$ [m/s]	Stochastic $\Delta v$ , $3\sigma$ [m/s]	Margin
$\Delta v_0$	8.3		5%
$\Delta v_1$ - $\Delta v_5$	129.2		5%
TCM		18	100%
HIM	12.2		5%
1-year SK		2.5	5%
Disposal	2		100%
<b>Total, without margins [m/s]</b>			<b>172.2</b>
<b>Total, margined [m/s]</b>			<b>199.8</b>

#### 4. Spacecraft design: from Phase 0 to Phase A

The design of the LUMIO spacecraft is currently ongoing its third iteration during the Phase A study. The first iteration was represented by the design proposed in response to the SysNova LUCE challenge, while the second iteration was obtained by including the modifications suggested by ESA's CDF study. Figure 4 shows the LUMIO spacecraft configuration proposed at the end of the challenge study: the changes introduced by the two successive iterations, although having some influence on the shape, size, placement in the spacecraft and choice of components of some of the sub-systems, have not drastically modified the layout shown in the figure. The margined wet spacecraft mass in the challenge study configuration was around 21 kg, later updated into 22.8 kg by the CDF study, mainly due to the introduction of a limited number of additional redundancies and to a 27% increase in the Delta-V budget.

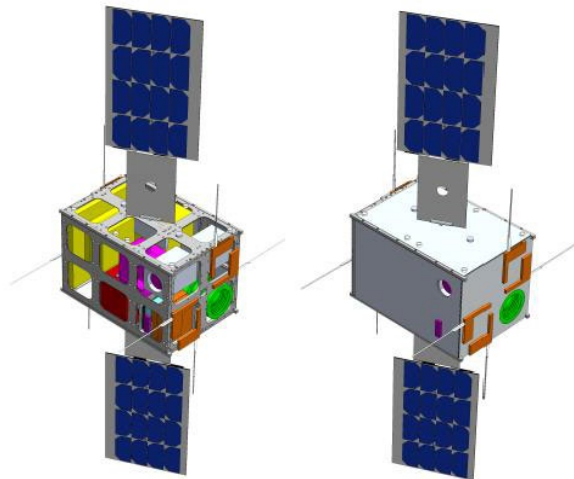


Fig. 4. LUMIO spacecraft configuration proposed at the end of the challenge study.

The following sub-sections provide an overview of the design status of all spacecraft sub-systems, highlighting the evolution of their design through the various iterations. A summary of this info is given, in a more concise way, in Table 3. Note that, for the Phase A design, the table shows only the number and type of COTS components, since a detailed trade-off for the actual supplier and model of each component is currently ongoing and has not been closed yet.

##### 4.1 Payload (LUMIO-Cam)

The LUMIO-Cam is a custom payload developed by one of the key partners of the LUMIO team, Leonardo. In its initial configuration as proposed in the design challenge, the LUMIO-Cam employed one single CCD201 detector with 1024x1024 active pixels, associated to an optics with a Field of View of 6 deg

and 127 mm focal length. The sensitivity of the chosen detector extends from visible to near-infrared spectrum, thus allowing for a wide range of exploitation of the impact radiation emissions.

The CDF study suggested some important improvements to this initial design. The most important change was represented by the introduction of an additional CCD201 detector, with a beam splitter allowing for dividing the incoming signal in two channels, a visible and a near-infrared one, detected by two separate sensors. Another important change was the introduction of a longer baffle in order to reduce the straylight effects and improve the quality of the detected signal. It was suggested to use for this baffle the maximum possible length allowed by the spacecraft configuration (160 mm). The resulting margined mass budget estimated for this modified camera configuration was around 2.1 kg.

The current detailed Phase A design of the LUMIO-Cam is based on these CDF recommendations, thus including two detectors and a beam splitter. Different baffle lengths up to 100 mm are being considered, and attention is also being given to the structural interfacing of the payload with the spacecraft. A CAD rendering of the current camera design is shown in Fig. 5.

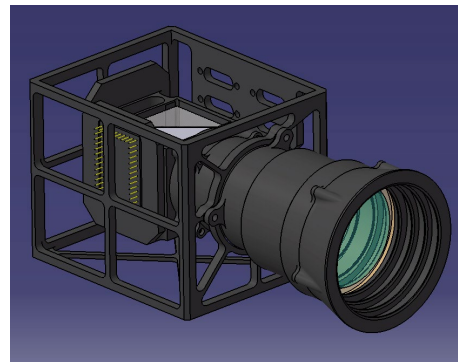


Fig. 5. CAD rendering of the current LUMIO-Cam design.

##### 4.2 Attitude Determination and Control System (ADCS)

The ADCS design is of crucial importance for the success of the LUMIO mission, given the constraints generated by the need for accurately pointing the LUMIO-Cam towards the Moon (for good-quality science product), the antennas towards the Earth (for communications and radiometric navigation) and the solar panels towards the Sun (for maximizing power generation). Especially the last constraint is particularly challenging for LUMIO, since in the operative orbit the Sun will continuously move with respect to the body-fixed reference frame of the spacecraft. This requires simultaneous pointing of the LUMIO-Cam towards the Moon and rotation of the solar arrays in the body-fixed frame by means of a dedicated drive mechanism, as

schematically shown by the pointing strategy illustrated in Fig. 6.

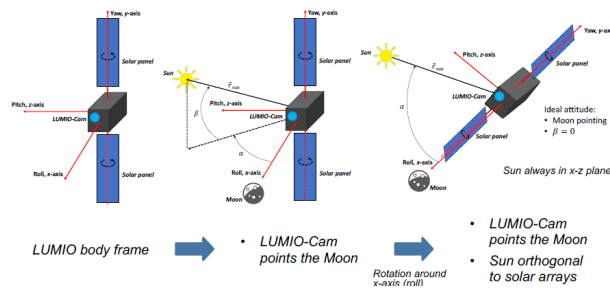


Fig. 6. LUMIO spacecraft pointing strategy.

In response to these needs, the initial challenge study proposed for the ADCS sensors two star trackers, two MEMS sun sensors and one IMU. The actuators were three reaction wheels, with desaturation performed by means of the propulsion system (as further explained in the following subsection).

The CDF study did not introduce significant changes to this design, limiting itself to remove the redundant star tracker, increase the redundancy on the sun sensors, and asking for a more frequent amount of wheel desaturation maneuvers (which also led to the selection of a different reaction wheel model).

No significant changes in the type of ADCS components are being made by the current Phase A study, which is however aiming at increasing the robustness of the design by introducing redundancies to avoid single points of failure on most of the components.

### 4.3 Propulsion

The initial propulsion system choice proposed in the challenge study was the VACCO Hybrid ADN MiPs system, which allowed to have in the same unit the main propulsion thruster (a 0.1 N mono-propellant) and four 10 mN cold gas thrusters in a “pyramid” configuration which, in that design, would have allowed for RCS maneuvers (de-tumbling and wheel desaturation). The available COTS options for this system were not sufficient in terms of Delta-V budget, therefore a customization of the system in terms of tank size and propellant mass was foreseen.

The CDF study proposed an alternative solution, mainly to overcome the uncertainties related to the customization of the VACCO system. In this case, the proposed propulsion design was based on two Aerojet MPS130-2U systems, mounted at two different corners of the spacecraft. This would allow for a total of eight 0.25 N mono-propellant thrusters at different locations, that can therefore be used for both main and RCS propulsion, depending on the amount of activated thrusters and their activation strategy.

Based on the lessons learned from Phase 0, the current Phase A study is considering two fully separate systems for the main and RCS propulsion. This allows for more flexibility, a larger number of potential COTS options offered by the market, and the possibility of separately optimizing the performance of the two systems. The main propulsion system will still be mono-propellant, with a maximum thrust level of 1 N, while both cold gas and electrothermal thrusters are being considered for the RCS part, with a thrust level in the range 1-10 mN.

### 4.4 Communications

The challenge study design of the LUMIO Telecommunications system was based on inter-satellite link with a Lunar orbiter, since Direct-to-Earth link was ruled out by the challenge constraints. This allowed to close the link with two UHF antennas, installed in turnstile configuration. However, the Direct-to-Earth option was put on the table again by the CDF study, which proposed a X-band design adaptable to both types of link.

The current phase A design is based on a number of further modifications for the Telecommunications system, mainly coming from the fact that radiometric navigation is now considered the baseline for the spacecraft, and the consequent increased demands in terms of data rate and link budget. The inter-satellite link option is still being considered, using the SSTL Lunar Pathfinder as relay spacecraft and two options for the frequency band (UHF and S-band). However, Direct-to-Earth link (either in the S- or X-band) is the current design baseline.

### 4.5 Data Handling

One of the main features of the LUMIO design is the presence of an On-Board Payload Data Processing unit (OBPDP), that allows to significantly reduce the amount of data to be sent to ground by limiting them to the scientifically significant data only. In order to do this, the OBPDP is designed in such a way to: (1) detect and keep only the camera images in which impact flashes are present; (2) cut from the whole image a smaller “tile”, including the flash area and the information on where this area is located on the Lunar farside surface as seen by the spacecraft. This data processing strategy, schematically summarized in Fig. 7, allows for a reduction by a factor in the order of  $10^6$  on the amount of data to be stored and sent to ground.



Fig. 7. LUMIO payload data processing strategy.

In the challenge study design, in order to allow for more robustness and redundancy, three separate OBC boards were included: the main spacecraft OBC, the OBDPD, and a dedicated one for the AOCS functions. In the CDF study and in the current Phase A study, however, given the relatively limited processing power required by the AOCS algorithms (around two order of magnitude smaller than the performance required by the OBDPD), it has been decided to combine the OBDPD and the AOCS functions in the same unit. The current Phase A design is mostly focusing on a further optimization of the on-board data processing algorithm, especially in terms of required processor power.

#### 4.6 Power

The design proposed by the challenge study was based on two solar array panels orientable by means of a SADA drive mechanism, plus two batteries for power storage. This allowed for an average power generation capability ranging from 22 W to 27 W during the various mission phases, and for a total battery storage capacity of 160 Wh.

The CDF study revised the power budget estimation made during the previous iteration, deriving an average power requirement of approximately 29 W in the LUMIO operative phase and up to 50 W in its transfer phase. As a consequence, the solar arrays were re-sized, with the addition of two more panels, in order to meet this increased power request.

The current Phase A study, as previously described, is based on a modified transfer phase strategy, as a consequence of the new launch opportunities that are being considered. This might eventually result in reducing again the power budget, to values closer to the ones that were estimated by the challenge study, and therefore modify the design choices in terms of number of solar panels required by the spacecraft.

#### 4.7 Structure

The spacecraft structure proposed by all design iterations, from the challenge study to the current Phase A design, is the 12U CubeSat structure developed by ISIS-Innovative Solutions In Space, which is also a member of the LUMIO team. The challenge study proposed the use of 1.5 mm Al panels for radiation hardening, but this analysis was considered excessively conservative by the CDF study, which recommended to revise it and eventually reduce the thickness and mass of the shielding panels. A more accurate radiation environment analysis is currently ongoing during Phase A, based on the latest mission analysis results for the

spacecraft orbit and trajectories, and on the use of the SPENVIS-NG and MULASSIS software packages.

#### 4.8 Thermal Control

The LUMIO thermal control system proposed by the challenge study was based on an extremely simplified thermal analysis of the spacecraft, which led to the adoption of a mostly passive control. A combined coating was proposed for the main CubeSat body, made of gold finishing (27%), silvered Teflon (25%) and polished Al 6061-T6 (48%). Black paint on an Al substrate was proposed for the back surfaces of the solar panels. In addition, three thermal resistors, with a power of 5 W each, were included for active local thermal control of the most critical spacecraft components.

A similar thermal design was proposed by the CDF study, with just small adjustments in terms of type and size of coatings. Similarly, the Phase A thermal control design of the spacecraft is not expected to deviate significantly from what has been proposed by the CDF and the challenge study.

### 5. Conclusions

The LUMIO mission, one of the winners of the ESA SysNova LUCE challenge, has the primary science goal to observe and characterize meteoroid impacts on the Lunar farside, in order to improve the current meteoroid models and reduce their currently existing areas of uncertainty. LUMIO complements, both in space and time, ground-based observations from other programs with its remote space-based ones, and is therefore expected to give an invaluable contribution to Lunar Situational Awareness. The LUMIO spacecraft will be a 12U CubeSat equipped with the LUMIO-Cam, an optical instrument capable of detecting impact flashes to continuously monitor and process the data. The mission implements a sophisticated transfer phase and orbit design, and will make use of the most advanced COTS CubeSat technology to serve as a demonstrator for the use of CubeSats as viable, low-cost platform for interplanetary science and exploration missions.

In this paper, the scientific relevance of LUMIO and its peculiar mission characteristics have been presented and discussed. The current LUMIO spacecraft design has been shortly introduced, highlighting its analogies and differences with the solutions proposed during Phase 0. The Phase A study of LUMIO is currently ongoing, and is scheduled for completion by the end of 2020.



Table 3. LUMIO spacecraft sub-systems: evolution from pre-phase 0 (SysNova challenge study) to Phase A.

	SysNova Challenge Study	ESA CDF Study	Phase A (current)
<b>Payload</b>	<ul style="list-style-type: none"> <li>• Custom (LUMIO-Cam)</li> <li>• EMCCD type, visible and near infrared spectrum</li> <li>• Single detector, CCD201</li> </ul>	<ul style="list-style-type: none"> <li>• Two CCD201 detectors, with common optics</li> <li>• Longer baffle (160 mm)</li> </ul>	<ul style="list-style-type: none"> <li>• Dioptic objective, 5 lenses</li> <li>• Beam splitter, two CCD201 detectors</li> <li>• Three baffle options: zero-sized, half-sized (50 mm), full-sized (100 mm)</li> </ul>
<b>ADCS</b>	<ul style="list-style-type: none"> <li>• 3x reaction wheels (Blue Canyon RWP-100)</li> <li>• 2x sun sensors (Solarmems NanoSSOC D60)</li> <li>• 2x star trackers (Hyperion ST400)</li> <li>• 1x IMU (Sensoror STIM300)</li> </ul>	<ul style="list-style-type: none"> <li>• 3x reaction wheels (Gomspace GSW600)</li> <li>• 4x sun sensors (Solarmems NanoSSOC D60)</li> <li>• 1x star trackers (Hyperion ST400)</li> <li>• 1x IMU (Sensoror STIM300)</li> </ul>	<ul style="list-style-type: none"> <li>• 4x reaction wheels</li> <li>• 3x fine sun sensors</li> <li>• 3x coarse sun sensors</li> <li>• 2x star trackers</li> <li>• 1x IMU</li> </ul>
<b>Propulsion</b>	<ul style="list-style-type: none"> <li>• Delta-V budget = 154.4 m/s</li> <li>• VACCO Hybrid ADN MiPS (customized)</li> <li>• Main: 1x 0.1 N mono-prop</li> <li>• RCS: 4x 10 mN cold gas</li> </ul>	<ul style="list-style-type: none"> <li>• Delta-V budget = 195.8 m/s</li> <li>• 2x Aerojet MPS130-2U</li> <li>• 8x 0.25 N mono-prop thrusters (for both main and RCS propulsion)</li> </ul>	<ul style="list-style-type: none"> <li>• Delta-V budget = 199.8 m/s</li> <li>• Separate main/RCS systems</li> <li>• Main: mono-prop, 1 N max.</li> <li>• RCS: 6-12x, cold gas or electrothermal, 1-10 mN</li> </ul>
<b>Communications</b>	<ul style="list-style-type: none"> <li>• Inter-satellite link, no Direct-to-Earth</li> <li>• 2x UHF antennas, turnstile</li> <li>• 1x UHF transceiver, based on CCSDS Proximity-1</li> </ul>	<ul style="list-style-type: none"> <li>• Both inter-satellite and Direct-to-Earth links</li> <li>• 4x patch antennas (X-band)</li> <li>• 1x Syrlinks EWC27-31 transceiver (customized)</li> </ul>	<ul style="list-style-type: none"> <li>• Baseline: Direct-to-Earth link (S- or X-band)</li> <li>• Optional: inter-satellite link (UHF or S-band)</li> </ul>
<b>Data Handling</b>	<ul style="list-style-type: none"> <li>• Three separate OBC (main/payload/AOCS)</li> <li>• Main: AAC Microtec Sirius</li> <li>• Payload/AOCS: 2x Gomspace Z7000</li> </ul>	<ul style="list-style-type: none"> <li>• Merged AOCS/payload boards</li> <li>• Main: Skylabs, Microsemi FPGA processing unit</li> <li>• Payload and AOCS: UniBAP e2000</li> </ul>	<ul style="list-style-type: none"> <li>• Merged AOCS/payload boards</li> <li>• Similar design as previous iterations</li> <li>• Optimization of on-board data processing algorithm</li> </ul>
<b>Power</b>	<ul style="list-style-type: none"> <li>• 2x Gomspace panels-B type</li> <li>• IMT SADA Assembly</li> <li>• 2x Gomspace BPX batteries</li> <li>• Gomspace P60 EPS</li> </ul>	<ul style="list-style-type: none"> <li>• 4x Gomspace panels-B type</li> <li>• IMT SADA Assembly</li> <li>• 2x Gomspace BPX batt.</li> <li>• Gomspace P60 EPS</li> </ul>	<ul style="list-style-type: none"> <li>• Similar design as previous iterations</li> <li>• Possible power budget reduction due to the modified transfer strategy</li> </ul>
<b>Structure</b>	<ul style="list-style-type: none"> <li>• ISIS 12U structure</li> </ul>	<ul style="list-style-type: none"> <li>• ISIS 12U structure</li> </ul>	<ul style="list-style-type: none"> <li>• ISIS 12U structure</li> </ul>
<b>Thermal</b>	<ul style="list-style-type: none"> <li>• Custom coating for main body and solar panels</li> <li>• 3x thermal resistors (5 W)</li> </ul>	<ul style="list-style-type: none"> <li>• 15 W heating power</li> <li>• Secondary surface mirror, black paint, gold finishing</li> </ul>	<ul style="list-style-type: none"> <li>• Similar design as previous iterations</li> </ul>

### Acknowledgements

The work described in this paper has been funded by the European Space Agency under the General Support Technology Programme (GSTP) and has received support from the national delegations of Italy (ASI), the Netherlands (NSO) and Norway (NOSA). The authors would like to particularly acknowledge the contribution of the ESA CDF team in reviewing and iterating the Phase 0 LUMIO design.

The input received from external experts throughout the LUMIO design process has been extremely valuable and their role is highly appreciated.

Finally, the authors would like to thank all the students and former members of the LUMIO team, who have given invaluable contributions to the mission design, especially in its early phases.

## References

- [1] European Space Agency, 2016, “SysNova: R&D Studies Competition for Innovation. AO#4: LUNar CubeSats for Exploration (LUCE)”, Statement of Work - Issue 1, Rev 0. TEC-SY/84/2016/SOW/RW
- [2] European Space Agency, 2018, “LUMIO. Review of SysNova Award LUMIO Study”, CDF Study Report CDF R-36
- [3] S. Speretta, et al., 2019, “LUMIO: an Autonomous CubeSat for Lunar Exploration”, in *Space Operations: Inspiring Humankind’s Future*, Springer nature Switzerland AG
- [4] P. Sundaramoorthy, et al., 2018, “System Design of LUMIO: a CubeSat at Earth-Moon L2 for Observing Lunar Meteoroid Impacts”, IAF 69th International Astronautical Congress, Bremen, Germany
- [5] F. Topputo, et al., 2018, “LUMIO: a CubeSat at Earth-Moon L2”, The 4S Symposium, Sorrento, Italy
- [6] [www.minorplanetcenter.net](http://www.minorplanetcenter.net) (last accessed: 30/9/20)
- [7] [cneos.jpl.nasa.gov](http://cneos.jpl.nasa.gov) (last accessed: 30/9/20)
- [8] Z. Ceplecha, et al., 1998, “Meteor Phenomena and Bodies”, *Sp. Sci. Rev.*, vol. 84, no. 3, pp. 327–471
- [9] E.J. Speyerer, et al., 2016, “Quantifying crater production and regolith overturn on the Moon with temporal imaging”, *Nature* 538.7624, pp. 215–218
- [10] J. Oberst, et al., 2012, “The present-day flux of large meteoroids on the lunar surface--A synthesis of models and observational techniques”, *Planet. Space Sci.*, vol. 74, no. 1, pp. 179–193
- [11] L. R. Bellot Rubio, et al., 2000, “Luminous Efficiency in Hypervelocity Impacts from the 1999 Lunar Leonids”, *Astrophys. J. Lett.*, vol. 542, no. 1, pp. L65--L68
- [12] R. M. Suggs, et al., 2008, “The NASA Lunar Impact Monitoring Program”, *Earth. Moon. Planets*, vol. 102, no. 1, pp. 293–298
- [13] A. Z. Bonanos, et al., 2015, “NELIOTA: ESA’s new NEO lunar impact monitoring project with the 1.2m telescope at the National Observatory of Athens”, *Proceedings of the International Astronomical Union*, vol. 10, no. S318, pp. 327–329
- [14] J.L. Ortiz, et al., 2006, “Detection of sporadic impact flashes on the Moon: Implications for the luminous efficiency of hypervelocity impacts and derived terrestrial impact rates”, *Icarus* 184.2, pp. 319–326
- [15] R.M. Suggs, et al., 2014, “The flux of kilogram-sized meteoroids from lunar impact monitoring”, *Icarus* 238.Supplement C, pp. 23–36